Protein Adsorption Kinetics Drastically Altered by Repositioning a Single Charge

J. J. Ramsden,*,†,‡ D. J. Roush,§,⊥ D. S. Gill,§,∥ R. Kurrat,‡,▽ and R. C. Willson§

Contribution from the Department of Biophysical Chemistry, Biocenter of the University of Basel, 4056 Basel, Switzerland, Department of Chemical Engineering, ETH, 8092 Zurich, Switzerland, and Department of Chemical Engineering, University of Houston, Houston, Texas 77204

Received March 17, 1995[⊗]

Abstract: A sterically conservative, neutralizing mutation (glutamic acid to glutamine) in either of two different positions (15 or 48) of the soluble core tryptic fragment of cytochrome *b*5 results in two proteins with vastly different adsorption properties. The kinetics of adsorption were measured under well-defined hydrodynamic conditions on a variety of different surfaces, of controlled electrostatic potential, prepared by modifying planar optical waveguides. Repeated measurement of the guided mode spectrum in the presence of protein solution allowed the temporal evolution of the number of adsorbed molecules to be determined. A highly positively charged surface acted as a perfect sink, i.e., adsorption was only limited by transport, adsorption to a highly negatively charged surface was fully reversible, and adsorption to a neutral phospholipid bilayer was very slow and practically irreversible. The macroscopic adsorption behavior can in large part be interpreted in terms of molecular-scale interactions between the protein and the adsorbent surface.

Introduction

Despite decades of interest and investigation, protein adsorption at the solid−liquid interface is still not generally understood. The elucidation of molecular mechanisms of the adsorption process will have impacts on fields as diverse as chromatography, immunoassays, biocompatibility, etc. It is only rather recently that methods have been developed for investigating the phenomenon of adsorption kinetics with sufficient precision for use in mechanistic investigations.[1] Because, in the great majority of cases encountered, adsorption is either irreversible or only partly reversible,[2] measurement of the kinetics of the process is an essential complement to equilibrium studies.

In unraveling mechanisms, there is a distinct advantage in being able to independently manipulate both the protein and the surface in detailed, specific ways. The results of such experiments provide rigorous tests for theories of adsorption. Here we report that a conservative charge rearrangement dramatically affects the adsorption behavior of the soluble tryptic core fragment of cytochrome *b*5 on a variety of surfaces.

Experimental Section

Surfaces. Adsorbing surfaces of controlled charge density were fabricated on 16 × 48 mm pyrolyzed sol−gel planar optical waveguides made from SiO_2 and TiO_2,[3] intimately mixed in the molar ratio 62:38.[4] This material is representative of a wide range of amphoteric oxides used in chromatography, etc. The thin (~170 nm), high refractive index (~1.8) waveguiding film is supported on Schott AF45 glass, and incorporates a 2 mm wide diffraction grating (period Λ = 416.15 nm, depth ~20 nm), produced by embossing before pyrolysis.[5] Waveguides (Artificial Sensing Instruments, Zurich, Switzerland, type 2400) were presoaked overnight in the buffer solution (0.01 M *N*-(2-hydroxyethyl)piperazine-*N*′-2-ethanesulfonic acid (HEPES)−NaOH, pH 7.2, plus 0.5 mM EDTA), which was used throughout the measurements.

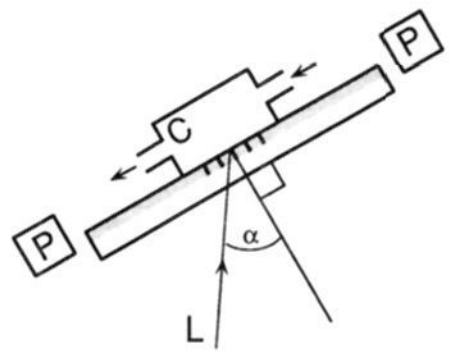

Figure 1. Schematic diagram of the measuring apparatus. The flow-through cuvette (C) is shown mounted on the waveguide. Photodiodes (P) record the power of the incident light (L) incoupled into the waveguide with angle α.

Mode Spectrum Measurements. Thin waveguides exhibit a discrete spectrum of modes, whose eigenvalues N depend on the reflectance of the waveguide−solution interface.[6,7] By directing a linearly polarized light beam (He−Ne laser, diameter 0.8 mm, wavelength λ = 632.816 nm) onto the grating coupler while varying the angle of incidence, the mode spectrum appears as a series of peaks in the power of light coupled into the waveguide,[8] measured using photodiodes positioned at the ends of the waveguide (Figure 1). The spectrum was recorded using an IOS-1 instrument (Artificial Sensing Instruments, Zurich, Switzerland) which has an angular resolution of ±1.25 μrad. N is related to the angle α corresponding to peaks in the spectrum according to

$$N = n \sin \alpha + l\lambda/\Lambda \qquad (1)$$

where n is the refractive index of air and l the diffraction order.

* To whom correspondence should be addressed.
† Biocenter of the University of Basel.
‡ ETH.
§ University of Houston.
⊥ Current address: Bioprocess R & D, Merck & Co., P.O. Box 2000, Rahway, NJ.
∥ Current address: Department of Surgery, Massachusetts General Hospital, and Harvard Medical School, Boston, MA 02114.
▽ Current address: Surface Technology, ETH, 8092 Zurich, Switzerland.
⊗ Abstract published in *Advance ACS Abstracts,* August 1, 1995.

(1) Ramsden, J. J. *J. Stat. Phys.* **1993**, *73*, 853−877.
(2) Kurrat, R.; Ramsden, J. J. *J. Chem. Soc., Faraday Trans.* **1994**, *90*, 587−590.
(3) Herrmann, P. P.; Wildmann, D. *IEEE J. Quantum Electron.* **1983**, *QE-19*, 1735−1738.
(4) Ramsden, J. J. *J. Mater. Chem.* **1994**, *4*, 1263−1265.
(5) Lukosz, W.; Tiefenthaler, K. *Opt. Lett.* **1983**, *8*, 537−539.
(6) Ghatak, A.; Thyagarajan, K. *Optical Electronics*; Cambridge University Press: Cambridge, 1989.
(7) Tien, P. K. *Rev. Mod. Phys.* **1977**, *49*, 361−420.
(8) Tiefenthaler, K.; Lukosz, W. *J. Opt. Soc. Am. B* **1989**, *6*, 209.

0002-7863/95/1517-8511$09.00/0

A small tubular flow-through cuvette of semicircular cross-section (equivalent hydrodynamic radius $R = 1$ mm, cross-sectional area $A = 1.6$ mm^2) made of silicone rubber (Wacker-Chemie, Munich, Germany, type RTV-M 533) passivated by repeated cycles of exposure to protein and extensive rinsing was mounted on the Si(Ti)O_2 surface of the waveguide, which thus formed one wall of the cuvette (Figure 1). The distance x from the inlet of the cuvette to the center of the measuring beam was 3.5 mm. Following establishment of a stable baseline with pure buffer flowing through the cuvette, flow was switched to protein at a bulk concentration c_b of 10 μg/cm^3 = 5.65 × 10^{14} molecules/cm^3 (this concentration was used in all experiments). Solutions were drawn through the cuvette by a downstream peristaltic pump at a flow rate $\mathcal{F}$ of 1.36 ± 0.15 mm^3/s. Temperature was monitored by a Pt-100 resistance thermometer embedded in the aluminum waveguide mounting, and was maintained at 25.5 ± 0.5 °C by keeping the entire apparatus and all solutions inside a constant temperature enclosure. The signal/noise ratio of the IOS-1 apparatus allows 2.5 × 10^8 adsorbed molecules to be detected in the detection area (defined by the extent of the incident laser beam) of 0.5 mm^2 (i.e., less than 0.1% of a monolayer of protein).

Proteins. Recombinant mutants E15Q and E48Q[9] of soluble rat cytochrome *b*5, the structures of which have been well characterized,[10,11] were prepared in *Escherichia coli* using synthetic genes generously given by Dr. Stephen Sligar of the University of Illinois.[12] Proteins were purified by ion exchange and size exclusion chromatography, and characterized using SDS–PAGE, spectrophotometry, and HPLC as described elsewhere.[12-14] Capillary isoelectric focusing using a 270A capillary electrophoresis system (Applied Biosystems, Foster City, CA) gave point of zero charge (pzc) values of 4.97 ± 0.10 and 4.95 ± 0.10 for E15Q and E48Q, respectively, i.e., identical within experimental error. The buffer pH (7.2) is therefore 2.2 units higher than the pzc. A simple explicit formula for the net charge Z per molecule is provided by the Linderstrøm–Lang equation[15,16]

$$Z = C - \sum_i (1 + \eta_i)^{-1} \tag{2}$$

where C is the number of cationic groups (19 in the case of our proteins) and η_i is defined by

$$\log \eta_i = \mathrm{p}K_i - \mathrm{pH} - \frac{Zq^2}{2.303\epsilon k_B T}\left(\frac{1}{R} - \frac{\kappa}{1 + \kappa(R + r)}\right) \tag{3}$$

where K_i is the protonation constant of the ith residue. The sum in eq 2 is taken over all the charged residues, for which standard pK values were used,[17] and including the two heme propionates (pK_a = 4.5). R is the radius of the equivalent sphere of the protein (1.6 nm for cytochrome *b*5) and r the radius of an ion (0.25 nm); κ is the reciprocal Debye length, equal to 0.33 nm^{-1} for our buffer. q is the elementary charge, ϵ the permittivity of the buffer (taken to be that of pure water), k_B Boltzmann's constant, and T the absolute temperature. Using this equation, the pzc was predicted to be 4.95, in good agreement with the experimental determination, and Z at pH 7.2 equal to $-6.57q$. It is also useful to have an empirical equation for Z. This was constructed by fitting the calculated Z values to a double logistic equation:

$$Z = q\left(19 - \frac{27}{1 + \exp(-\beta(\mathrm{pH} - 3.7))} - \frac{16}{1 + \exp(-\beta(\mathrm{pH} - 12.6))}\right) \tag{4}$$

with $\beta = 0.7547$.

Experimental Data Analysis. Zero-order transverse electric (TE) and transverse magnetic (TM) modes were excited and α was measured every 27 s. From the N_{TE} ($\varrho = 0$) and N_{TM} ($\varrho = 1$) values, simultaneous solution of the mode equations[1,8]

$$\frac{2\pi}{\lambda}(n_F^2 - N^2)^{1/2}\left(d_F + d_A\frac{n_A^2 - n_C^2}{n_F^2 - n_C^2}\left[\frac{(N/n_C)^2 + (N/n_A)^2 - 1}{(N/n_C)^2 + (N/n_F)^2 - 1}\right]^{\varrho}\right) = \arctan\left[\left(\frac{n_F}{n_S}\right)^{2\varrho}\left(\frac{N^2 - n_S^2}{n_F^2 - N^2}\right)^{1/2}\right] + \arctan\left[\left(\frac{n_F}{n_C}\right)^{2\varrho}\left(\frac{N^2 - n_C^2}{n_F^2 - N^2}\right)^{1/2}\right] \tag{5}$$

yields the thickness d_A and refractive index n_A of the protein adlayer A. All the other parameters in eq 5 are known from prior measurement. The number ν of adsorbed proteins per unit area can be calculated from d_A and n_A according to[1]

$$\nu = \frac{d_A(n_A - n_C)}{m(\mathrm{d}n/\mathrm{d}c)} \tag{6}$$

where n_C is the refractive index of the buffer (1.331 67 at 25.5 °C and 632.8 nm), m the mass per protein molecule (1.77 × 10^{-14} μg), and dn/dc the refractive index increment of the protein (1.63 × 10^5 cm^3/μg at 25.5 °C and 632.8 nm). The buffer refractive index and protein refractive index increments were measured using an LI3 Rayleigh interferometer (Carl Zeiss, Jena, Germany). The refractive index increment has been found to remain constant up to protein concentrations of 400 mg/cm^3.[18]

Note that the measurement of two quantities (in our case d_A and n_A) allows ν to be calculated with fewer assumptions than other methods also currently used, e.g., surface plasmon resonance.[19] Our method is therefore more robust.

Preparation of Surfaces. Defined surfaces of differing charge densities were deposited on the waveguides using Langmuir–Blodgett and other techniques prior to protein adsorption. To produce a plain Si(Ti)O_2 surface, the surface was cleaned by being immersed for 30 min in hot (100 °C) concentrated Caro's acid (H_2SO_5). A strongly positively charged surface was produced by depositing a thin layer of poly(allylamine) (Aldrich, "high molecular weight") onto the waveguide.[20] To produce a strongly negatively charged surface, four layers of stearic acid (Sigma) were deposited in the "Y" configuration (i.e., head-to-head and tail-to-tail, with the outermost layer facing the solution composed of carboxylate groups) at a surface pressure of 20 mN/m from an aqueous subphase containing 5 × 10^{-4} M $BaCl_2$ using standard Langmuir–Blodgett techniques.[21] A neutral surface was prepared by depositing a bilayer of synthetic 1-palmitoyl-2-oleyl-*sn*-glycero-3-phosphocholine (POPC; Avanti Polar Lipids, Alabaster, AL) at a surface pressure of 32 mN/m from the buffer subphase onto the waveguide using a combination of the Langmuir–Blodgett and Langmuir–Schaefer techniques.[22]

Estimation of the Surface Charge Density. For monoprotic acidic or basic groups present at a density N_s on a surface, we have[23]

$$\mathrm{pH} - \mathrm{p}K_a = -\frac{\gamma}{2.303} \pm \log\left(\frac{\pm\gamma}{\sinh(\gamma/2)} - 1\right) \tag{7}$$

(9) E15Q is interpreted as glutamic acid (E) mutated to glutamine (Q) at position 15. This representation employs the standard IUPAC 1-letter codes for amino acids.

(10) Gill, D. S.; Roush, D. J.; Willson, R. C. *J. Biomol. Struct. Dyn.* **1994**, *11*, 1003–1015.

(11) Mathews, F. S.; Czerwinski, E. W. In *The Enzymes of Biological Membranes*; Martonosi, A. M., Ed.; Plenum: New York, 1983; Vol. 4, Chapter 52.

(12) von Bodman, S. B.; Schuler, M. A.; Jollie, D. R.; Sligar, S. G. *Proc. Natl. Acad. Sci. U.S.A.* **1986**, *83*, 9443–9447.

(13) Gill, D. S.; Roush, D. J.; Willson, R. C. *J. Colloid Interface Sci.* **1994**, *167*, 1–7.

(14) Roush, D. J.; Gill, D. S.; Willson, R. C. *J. Chromatogr.* **1993**, *653*, 207–218.

(15) Kuramitsu, S.; Hamaguchi, K. *J. Biochem.* **1980**, *87*, 1215–1219.

(16) The Linderstrøm–Lang equation is only an approximation. Nevertheless, as Kuramitsu and Hamaguchi have pointed out,[15] the results are remarkably good and have the advantage of computational simplicity.

(17) Dawson, R. M. C.; Elliott, D. C.; Elliott, W. H.; Jones, K. M. *Data for Biochemical Research*, 3rd ed.; Oxford University Press: Oxford, 1986.

(18) de Feijter, J. A.; Benjamins, J.; Veer, F. A. *Biopolymers* **1978**, *17*, 1759.

(19) Ramsden, J. J. *Q. Rev. Biophys.* **1994**, *27*, 41–105.

(20) Ramsden, J. J.; Lvov, Yu. M.; Decher, G. *Thin Solid Films* **1994**, *254*, 246–251.

(21) Roberts, G. G., Ed. *Langmuir-Blodgett Films*; Plenum: New York, 1990.

(22) Ramsden, J. J. *J. Phys. Chem.* **1993**, *97*, 4479–4483.

(23) Healy, T. W.; White, L. R. *Adv. Colloid Interface Sci.* **1978**, *9*, 303–345.

Table 1. PhysicoChemical Characterization of the Surfaces

parameter	polyallylamine	POPC	$Si(Ti)O_2$	stearate
W^a/nm	1.5[b]	0.1	0.09	0.04[c]
pK_a	10.8			5.4[d]
pH_0			2.5,[e,i] 5.8[e,j]	
ΔpK			7.0,[e,i] 2.0[e,j]	
N_s/nm^{-2}	6.5[f]		1.5,[e,i] 5.0[e,j]	6.5[f]
ψ_0/mV	219	0.0	−95[g]	−156
$\sigma_0/(\mu C\ cm^{-2})$	44	0.0	−3.7[g]	−13
pH_s	10.9	7.2	5.6	4.5
Z/q	−10.9	−6.6	−2.0	1.6
E15Q[h]	740	12.2	470	230
E48Q[h]	740	2.6	60	180

[a] Surface roughness defined as $W^2 = \sum_i^M (h_i - \langle h \rangle)^2/M$, where h_i is the height of the ith out of M sample points. The figures quoted were measured by atomic force microscopy. [b] Preliminary characterization (Yu. M. Lvov, personal communication). [c] Some restructuring of the surface takes place to produce islands of varying heights.[25] The figure quoted refers to single islands, which have exceedingly smooth surfaces. [d] From ref 26. [e] From ref 23. [f] Estimate. [g] Weighted mean for the mixed oxide $Si_{0.62}Ti_{0.38}O_2$. [h] Initial rate of adsorption in units of molecules $\mu m^{-2}\ s^{-1}$. [i] For SiO_2. [j] For TiO_2.

where $y = \psi e/(k_B T)$ is the dimensionless form of the surface potential ψ and γ is another dimensionless parameter consolidating surface site density and electrolyte concentration effects, defined by $\gamma = N_s\kappa/(4c_e)$, c_e being the bulk electrolyte concentration.[24] In eq 7, the plus signs are to be taken for a basic surface and the minus signs for an acidic surface. The surface potential determines the pH in the vicinity of the surface, pH_s:[23]

$$pH_s = pH + y/2.303 \tag{8}$$

Once ψ has been determined, the surface charge density σ_0 can be calculated from the familiar Gouy–Chapman expression

$$\sigma = \frac{2\epsilon\kappa k_B T}{q} \sinh \frac{y}{2} \tag{9}$$

For the amphoteric $Si(Ti)O_2$ surface the corresponding expression is[23]

$$\frac{\sinh y/2}{\gamma} = \frac{\delta \sinh \xi}{1 + \delta \cosh \xi} \tag{10}$$

where $\delta = 2 \times 10^{-\Delta pK/2}$ and $\xi = 2.303\Delta pH - y$, where $\Delta pH = pH_0 - pH$, pH_0 being the isoelectric point of the material. The surface potential was calculated separately for pure SiO_2 and TiO_2 and the appropriately weighted mean taken for the mixed oxide. The electrostatic parameters of the various surfaces are given in Table 1.

Results

Overview. As soon as protein flow is initiated (at $t = 0$), adsorption begins. From the monotonic diminution in the rate of deposition which was observed in every case, we conclude that only a monolayer of protein is deposited, and as the surface fills up deposition comes to a halt. Qualitatively, we note agreement of the results with the naive prediction that the positively charged surface (poly(allylamine)) should give faster adsorption, ending at a higher plateau, than the neutral or negatively charged surfaces. The order of rates was poly(allylamine) > $Si(Ti)O_2$ ≈ stearate > POPC. Saturation coverage was only attained with poly(allylamine); in the case of $Si(Ti)O_2$ and POPC the adsorption rates were much too slow for saturation to be approached on the time scale of the experiments. On the stearate surface an equilibrium coverage determined by the ratio of the on and off rates was rapidly attained. Hence, adsorption to a negatively charged surface (stearate and $Si(Ti)O_2$) is enhanced compared with that to neutral (zwitterionic) POPC.

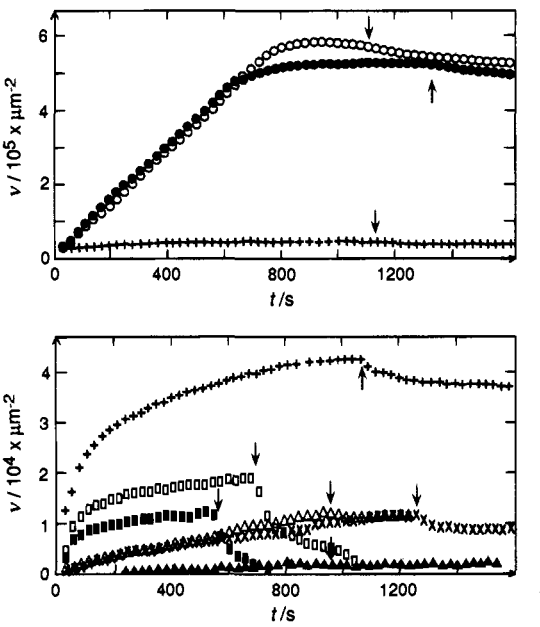

Figure 2. (a) Kinetics of adsorption of E15Q (○) and E48Q (●) to poly(allylamine). For comparison, E15Q adsorbing to POPC (+) is also shown (see also part b). Arrows show when protein flow was replaced by pure buffer. (b) Kinetics of adsorption of E15Q (+, □, △) and E48Q (■, ×, ▲) to $Si(Ti)O_2$ (+, ×), stearate (□, ■), and POPC (△, ▲). Arrows show when protein flow was replaced by pure buffer.

E15Q always adsorbed better than E48Q; the ratios of the initial rates decreased in the order POPC ≈ $Si(Ti)O_2$ > stearate > poly(allylamine). In other words, the rate differences (related to chromatographic selectivity) are lowest for the highest-affinity system, poly(allylamine), which is typical of separation operations.

A further aspect is the extent to which adsorption could be reversed by replacing the protein solution with pure buffer (an arrow marks where this was done in the figures). The amounts of protein desorbed followed the order stearate (complete desorption) > $Si(Ti)O_2$ > POPC ≈ poly(allylamine) (insignificant desorption).

Quantitative Analysis. We formulate the following three questions: (1) How fast is the protein adsorbed and desorbed (with rates characterized by rate coefficients k_a and k_d, respectively)? (2) What limits the maximum amount adsorbed? (3) What is the molecular mechanism of adsorption (including identification of the forces involved)? Before extracting parameters from the data, we need models to describe the processes occurring. Inspection of Figure 2 suggests three different phenomenonological models (Figure 3): I, the surface is a perfect sink and all arriving proteins are irreversibly adsorbed (poly(allylamine));[27] II, adsorption is reversible and therefore attains an equilibrium (stearate); III, the protein can adsorb in both a reversible (subscript r) and an irreversible (subscript i) mode $(Si(Ti)O_2)$,[2] i.e., a combination of models I and II. The adsorption to POPC appears to be almost irreversible and resembles I, except that the rate of adsorption is about 100 times slower than to a perfect sink, as discussed below.[27]

(24) The derivation of this equation makes use of the Gouy–Chapman theory (eq 9) which, with its assumptions of point ions, uniform ϵ, etc., is not expected to hold precisely at high surface charge densities. The Gouy–Chapman approach has the strong advantage of permitting explicit, analytically soluble equations to be obtained, compared with possibly more accurate, but complicated, expressions (e.g., expression based on the nonlinear Poisson–Boltzmann equation).

(25) Schwartz, D. K.; Garnaes, J.; Viswanathan, R.; Zasadzinski, J. A. N. *Science* **1992**, *257*, 508–511.

(26) Yazdanian, Y.; Yu, H.; Zografi, G. *Langmuir* **1990**, *6*, 1093–1098.

(27) A very small amount of desorption was observed from both poly(allylamine) and POPC, but has been neglected in the analysis.

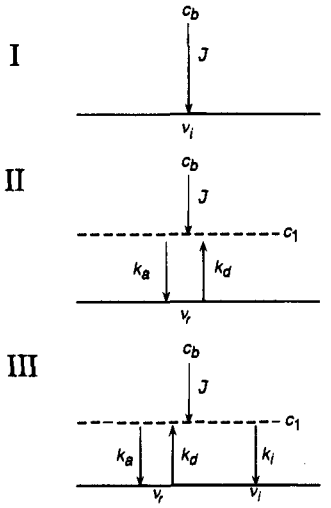

Figure 3. The three kinetic models referred to in the text. Subscripts r and i of ν refer to reversibly and irreversibly adsorbed proteins, respectively. The flux parameter J is given by the Nernst–Levich equation[32] $J = (c_b - c_1)D/\delta$, with δ given by eq 13. c_1 is set to zero for model I. The rate constants for reversible adsorption, desorption, and irreversible adsorption are k_a, k_d, and k_i, respectively.

Adsorption can be considered as a heterogeneous second-order reaction:[28]

$$d\nu/dt = \phi c_1(k_a + k_i) - \nu_r k_d \qquad (11)$$

where ϕ is the fraction of the area available for adsorption, and c_1, the protein concentration close to the surface, is obtained by summing fluxes to and from this near-surface layer and assuming $dc_1/dt \approx 0$; i.e.[2]

$$c_1 = \frac{c_b D/\delta + k_d \nu}{(k_a + k_i)\phi + D/\delta} \qquad (12)$$

where D is the translational diffusion coefficient of the protein in the bulk solution (1.6×10^{-6} cm^2/s)[29] and δ the thickness of the diffusion boundary layer, given by[32]

$$\delta = (3/2)^{2/3}(DxRA/\mathcal{F})^{1/3} \qquad (13)$$

where x, R, and A are the dimensions of the cuvette given earlier. This equation is valid for the laminar flow regime (in our experiments, the Reynolds number is about 1) in which the flux from the bulk to the layer in which the concentration is c_1 is determined by convective diffusion.

For a perfect sink (Figure 3, I), $\phi = 1$ and eq 11 becomes

$$d\nu/dt = c_b D/\delta \qquad (14)$$

This gives us the maximum possible rate of adsorption, 740 molecules μm^{-2} s^{-1}. Even in the absence of any energy barriers to adsorption, for monolayer deposition this rate can only be sustained at the very beginning when the adsorbing surface is completely empty. The random sequential addition of molecules to a continuum (i.e., a surface lacking discrete adsorption sites) results in gaps between adsorbed molecules too small to admit further molecules. Taking this effect into account results in the expression (valid up to $\nu a \approx 0.3$)[33]

$$\phi = 1 - 4\nu a + \frac{6\sqrt{3}}{\pi}(\nu a)^2 + b(\nu a)^3 \qquad (15)$$

where a is the area per adsorbed molecule. The constant b equals 1.43 for spheres adsorbing irreversibly and immovably and 2.40 where the surface configuration of the adsorbed (spherical) molecules is maintained at equilibrium through desorption–adsorption processes[33] or surface diffusion.[34]

Adsorption to poly(allylamine) is characterized by a constant rate of adsorption of 740 molecules μm^{-2} s^{-1} up to an extremely high surface loading of *ca.* 6×10^5 molecules μm^{-2}. This is precisely the maximum rate of convective–diffusive transport calculated above; i.e., poly(allylamine) is indeed a perfect sink for cytochrome *b*5 adsorption. Intriguingly, ϕ appears to remain equal to 1 until just before ν_{max} is reached, when the rate of adsorption falls rather abruptly.

As can be seen from Table 1, initially the surface charge is extremely positive and will strongly attract the negatively charged protein. Moreover pH_s is predicted (eq 8) to have a value of 10.9, at which the net charge Z per protein is about $-11q$. As adsorption proceeds, the initially positive surface charge σ_0 will be gradually neutralized by the negative protein. Writing the surface charge as

$$\sigma(t) = \sigma_0 + \nu(t)\, Z(\sigma) \qquad (16)$$

and eliminating $\sigma(t)$ and Z with eqs 9 and 4, we can solve for the surface potential ψ, and find a value of about -55 mV at the measured saturation value of *ca.* 6×10^5 protein molecules μm^{-2}. Evidently, the maximum loading is not limited by electrostatic neutralization of the surface, but by ϕ falling to zero. Although the rates of adsorption of E15Q and E48Q are identical until ν_{max} is almost attained, the actual saturation values differ slightly (5.75×10^5 and 5.12×10^5 molecules μm^{-2}, respectively). This may be a consequence of E15Q having a larger dipole than E48Q and hence a tendency to sit on the surface more rigidly, with less freedom to librate and sterically inhibit further occupancy.

Were the poly(allylamine) surface completely planar, the measured ν_{max} would correspond to a close-packed monolayer with each protein molecule occupying only 1.5 nm^2. This is ruled out by the actual geometry of the protein, which is an oblate spheroid with major and minor axes of 3.2 and 2.5 nm, respectively,[31] and which must therefore occupy a minimum area of about 6 nm^2 per molecule. The poly(allylamine) surface is not completely smooth, however, but has a roughness of *ca.* 1.5 nm as seen by using atomic force microscopy (see Table 1). Its capacity will therefore be greater. Comparison of the geometric minimum area with the measured area per molecule suggests that it is 6/1.5 = 4 times that of a smooth planar surface.

Adsorption to POPC. Qualitatively the behavior resembles that of adsorption to poly(allylamine) (i.e., described by model I) except that the rates of adsorption $d\nu/dt$ are much lower than the maximum rates (see Table 1). In contrast to poly(allylamine), to which every arriving molecule sticks, these

(28) This equation applies to model III of Figure 3, which is simply a combination of models I and II. The parameter $J = (c_b - c_1)D/\delta$ gives the net flux of molecules to the surface; in model I $J = d\nu/dt = c_b D/\delta$ (eq 14).

(29) Calculated using Perrin's formula,[30] recalling that cytochrome *b*5 is describable as an oblate spheroid with major and minor axes of 3.2 and 2.5 nm, respectively.[31]

(30) Perrin, F. *J. Phys. Radium (Ser. 7)* **1936**, *7*, 1–11.

(31) Archakov, A. I.; Bachmanova, G. I. *Cytochrome P450 and active oxygen*; Taylor & Francis: London, 1991.

(32) Levich, V. G. *Physicochemical Hydrodynamics*; Prentice-Hall: Englewood Cliffs, NJ, 1962.

(33) Schaaf, P.; Talbot, J. *J. Chem. Phys.* **1989**, *91*, 4401–4409.

(34) Surface diffusion of the adsorbed proteins is only likely to occur on the phospholipid bilayer. Unless it leads to clustering[35] of the adsorbed proteins, however, the increase from 1.4 to 2.4 in the value of b in eq 15 has a negligible effect on the adsorption kinetics.

(35) Ramsden J. J.; Bachmanova, G. I.; Archakov, A. I. *Phys. Rev. E* **1994**, *50*, 5072–5076.

Table 2. Fitted Parameters for Adsorption to Stearate Using Model II (See Figure 3)[a]

parameter	E15Q	E48Q	units
k_a	3.0×10^{-5}	2.5×10^{-5}	cm/s
k_d	9.2×10^{-3}	1.3×10^{-2}	s^{-1}
a	3.2	4.3	nm^2
$c_b k_a/k_d$	1.8×10^4	1.1×10^4	molecules μm^{-2}
ν_{max}[b]	1.85×10^4	1.3×10^4	molecules μm^{-2}

[a] ν_{max} corresponds to about 6% of a complete monolayer for both E15Q and E48Q. [b] Measured from the adsorption plateau (Figure 2).

figures signify that only 1 in 60 adsorption attempts resulted in adsorption, in the case of E15Q, and only 1 in 280 in the case of E48Q.[36] Despite these very low rates of adsorption, the results show that the adsorption nevertheless retains a highly specific character and is drastically affected by a single point mutation.

Phospholipid bilayer membranes in the liquid crystalline phase are fluid enough to undergo thermomechanical fluctuations, resulting in an additional repulsive force between two membranes approaching each other.[37] Since the persistence length of a POPC membrane at room temperature is much greater than the diameter of a protein molecule, however, we may neglect this possible source of protein−membrane repulsion.

Deposition onto Stearate (Model II). The stearate surface is initially highly negatively charged (Table 1) and is therefore expected to repel the negatively charged cytochrome *b*5. When we recalculate the surface potential at the adsorption plateau using eq 16, we find it almost unchanged at 156 mV for both E15Q and E48Q, despite their different equilibrium coverages (Table 2); i.e., the surface charge is extraordinarily well buffered. Insight into this behavior comes through calculating the actual charge of the protein as a function of the distance z from the surface. From the bulk the protein sees a repulsive force, which is nevertheless quite weak because the potential falls off exponentially with z according to the Gouy−Chapman expression $\psi(z) = \psi_{z=0} \exp(-\kappa z)$. As the protein approaches the surface the repulsive force would increase *were the protein charge to remain constant.* Since the surface is highly negatively charged, however, the local pH falls as the surface is approached (eq 8), and the charge on the protein changes accordingly. The surface pH is so low (Table 1) that at the surface the protein is predicted to have a net positive charge ($Z = +1.6q$). Therefore, as the protein moves from the bulk toward the surface, the initially repulsive force changes into an attractive one. Figure 4 shows plots of the electrostatic potential energy of the cytochrome *b*5 molecule, i.e., $\psi(z)\ Z(\psi)/(k_BT)$, with Z given by eqs 4 and 8, as it approaches highly charged surfaces.[38] For the extreme surface charge densities employed in this work, there is apparently no need to invoke the patch concept[39] to understand how a negatively charged protein can adsorb at a strongly negatively charged surface. Adsorption at less strongly charged surfaces, however, may involve clusters of residues of sign opposite that of the net protein charge.

The kinetic parameters for adsorption to stearate are collected in Table 2. ν_{max} is given by the quotient of k_a and k_d multiplied by the bulk concentration, i.e., 1.8×10^4 and 1.1×10^4 molecules/μm^2 for E15Q and E48Q, respectively. These values are in good agreement with the plateaus actually measured, suggesting that the model of a simple two-state process (adsorbed−desorbed) is correct. In contrast to adsorption to $Si(Ti)O_2$, the two mutants do not differ greatly from one another.

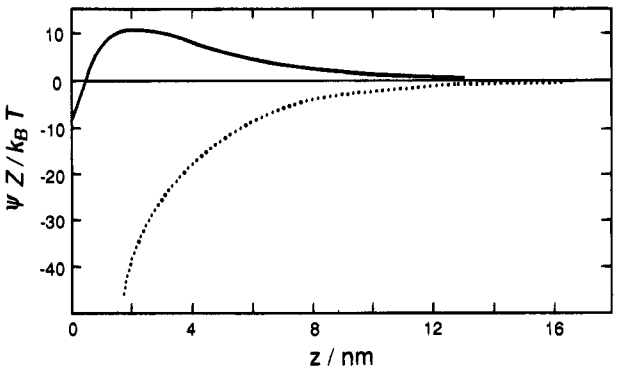

Figure 4. $\psi Z/(k_BT)$ for mutant cytochrome *b*5 approaching a poly(allylamine) surface (dotted line) and a stearate surface (solid line).

Table 3. Fitted Parameters Using Model III (See Figure 3) for Adsorption to $Si(Ti)O_2$

parameter	E15Q	E48Q	units
k_a	7.0×10^{-5}	4.8×10^{-6}	cm/s
k_d	8.2×10^{-3}	7.0×10^{-3}	s^{-1}
k_i	1.3×10^{-5}	1.5×10^{-6}	cm/s
a	7.5	14.1	nm^2

Adsorption to $Si(Ti)O_2$. We apply the model (III) developed previously[2] for albumin adsorbing to the same material. According to this model, there are two modes of adsorption, reversible and irreversible, with association rate constants k_a and k_i, respectively, and dissociation rates constants of k_d and zero. The fitted rate constants and a are given in Table 3. The difference in the molecular areas a occupied by the two mutants is especially intriguing. Cytochrome *b*5 is an oblate spheroid with major and minor axes of 3.2 and 2.5 nm.[31] The results suggest that E15Q adsorbs with its major axis perpendicular to the surface. The area measured for E48Q is too big to correspond to the alternative orientation, i.e., with the major axis parallel to the surface, and may correspond to a more flexible adsorption mode, in which librations enhance the effective area occupied, in accord with our expectation that the larger dipole moment of E15Q reduces the number of orientations likely to be found.

Structural Stability of Cytochrome b_5. The soluble core of cytochrome b_5 is a notably stable molecule. According to our differential scanning calorimetry (DSC) measurements, the unfolding temperature of the wild type protein exceeds 65 °C. The fractional recoveries of protein after long adsorption on the strong anion exchanger Mono Q, even at temperatures up to 30 °C, are routinely greater than 90%. The mutants have not been characterized by DSC, but also give excellent recoveries after HPLC.[40]

Literature observations on protein stability effects on adsorption pertain largely to equilibrium properties, and especially to the maximum extent of adsorption and desorbability. The initial rates of adsorption observed in the present work should be much less influenced by stability effects. Further, we would argue that proteins adsorbed on the stearate surfaces (from which complete desorption was observed) are not extensively denatured (we cannot exclude the possibility of slight, transient rearrange-

(36) The derivation of these numbers from the experimentally determined rate constants is discussed fully by J. J. Ramsden, G. I. Bachmanova, and A. I. Archakov, to be published.

(37) Helfrich, W. *Z. Naturforsch.* **1978**, *33a*, 305−315.

(38) This calculation assumes that there is no change in the conformation of the protein during its diffusion from the bulk pH region to the surface—which will take a time of $\sim(10\ nm)^2/D \approx 1\ \mu s$. This time may be too short even for the heme to dissociate from the rest of the protein, which occurs near its pzc.

(39) Roush, D. J.; Gill, D. S.; Willson, R. C. *Biophys. J.* **1994**, *66*, 1290−1300.

(40) Soluble cytochrome *b*5 shows no tendency to self-aggregate in NMR experiments even at 6 mM protein; this is unusually low stickiness.

ments, but believe that gross conformational changes would not be so readily reversed).

Conclusions

An integrated optical technique applied under controlled hydrodynamic conditions can be used to obtain accurate kinetics of the adsorption of mutant soluble (tryptic core) cytochrome *b*5 protein to various surfaces.

The electrostatic analysis presented here only permits a limited quantitative understanding of the ordering of the degrees of adsorption; i.e., adsorption to poly(allylamine) was faster than to $Si(Ti)O_2$, which was faster than to the most highly negatively charged surface, stearate. The desorption rates followed the inverse order; namely, adsorption was wholly reversible, partly reversible, and irreversible for stearate, $Si(Ti)O_2$, and poly(allylamine), respectively. Up to a very high surface loading (4 times the monolayer coverage predicted for a *smooth* planar surface) the poly(allylamine) layer acts as a perfect sink.

In both adsorption and desorption, however, the electrostatically neutral lipid bilayer (POPC) was anomalous: the rate of adsorption was the slowest, yet practically irreversible. In order to understand this phenomenon, polar and apolar interfacial forces need to be taken into account, as well as electrostatic ones.[41]

Furthermore, a simple analysis based on net charge is unable to account for the marked differences between the mutants, pointing to the need to take the actual surface charge distribution explicitly into account in the prediction of the adsorption and desorption behavior.

Acknowledgment. We thank Dr. Stephen Sligar (University of Illinois) for the genes encoding cytochrome *b*5 and its charge mutants and are grateful to the Human Frontier Science Program Organization, the Welch Foundation, and the National Science Foundation for grants to support this work. We thank Mr. Christoph Stürzinger for having determined the isoelectric points of the proteins and Mr. Gergely Antal and Miss Simone Karrasch for having taken the atomic force micrographs used to determine the surface roughnesses.

JA950885S

(41) van Oss, C. J.; Chaudhury, M. K.; Good, R. J. *Chem. Rev.* **1988**, *88*, 927−941.